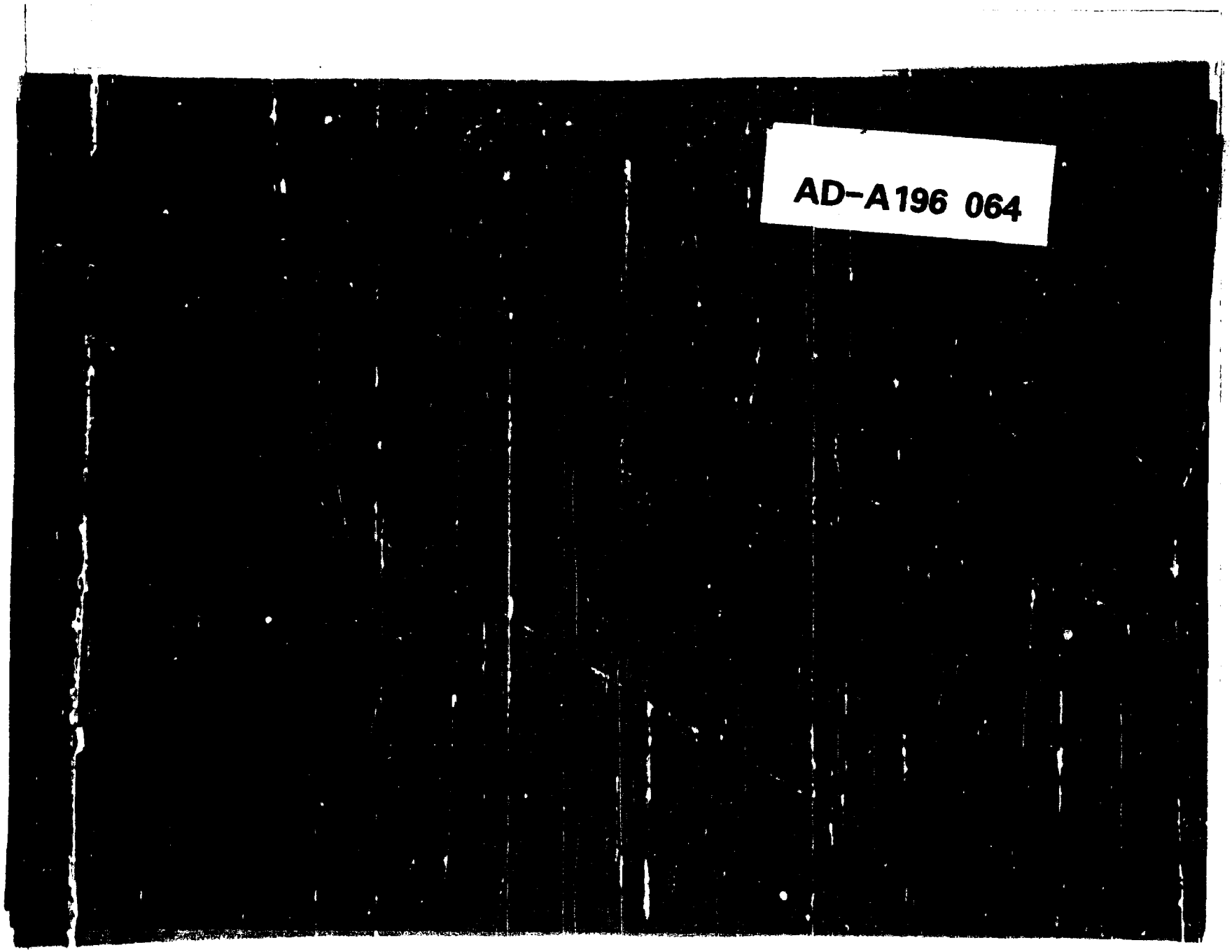

ROYAL AIRCRAFT ESTABLISHMENT

Technical Memorandum FS(F) 679

Received for printing 27 October 1987

A METHOD OF IMPROVING REMOTE REPRODUCTION OF A SOUND FIELD BY ONE-THIRD-OCTAVE ANALYSIS AND DIGITAL FILTERING

by

J. B. Collister

SUMMARY

This Memorandum describes work done to improve the measure of agreement between a target one-third-octave spectrum and its reproduction via some remote sound source. Digital filters create limited bandwidth data which are modified and finally recombined to produce a new time history. Studies of certain fixed and rotary wing aircraft have shown mean errors significantly reduced by this technique.

LIST OF CONTENTS

1 INTRODUCTION

A requirement in many ground-based experiments is the ability to establish a determinate sound pressure field in a chamber that can accommodate human subjects. Frequently, this field is required to approximate to that existing in some distant environment, such as an aircraft cockpit in flight.

A tape-recording of the time-history of, say, the cockpit noise can be obtained and may well represent to the ground-based observer the only available information on the frequency content of the source field. We may conveniently refer to this as the target field in both time and frequency domains.

However, on replay in the ground chamber, that tape-recording will not in general produce an exact duplication of the target field for many reasons: the multiple mechanical sources of the original noise and the acoustics of the cockpit cannot be precisely reproduced in a laboratory. Thus, frequency analysis equipment set up in the chamber during the time that some sound-reproduction equipment is replaying the target time history, will not display the target spectrum as existed in the aircraft, but rather an observed spectrum that differs from it by an error spectrum.

A typical third-octave error spectrum is shown in Fig 1a for a modern jet aircraft where the target field is that of whitish noise over the audible range of the spectrum; it is seen that deviations of ±10 dB exist.

A method has been developed whereby the error spectrum may be reduced considerably as seen in Fig 1b. The method is lengthy, even with the use of an Array Processor, but it has proved practicable in dealing with typical time histories of aircraft noise where the duration of some quasi-stable state of interest does not exceed 30 seconds or so.

Fig 1c&d are a comparable pair of error spectra for a noise source with significant deterministic frequencies present - they derive from a helicopter at the hover. Again, a considerable improvement is noted, this time extending down to the low harmonics of the blade-passing frequencies.

It has been observed that the revised aircraft noise markedly retains the character of the original noise, as opposed to that of totally synthetic random noise.

2 METHOD

2.1 Principle of method

The principle of the method is as follows. An observed time history is obtained by means of a microphone in the chamber, and this is analysed in real time by a B/K Frequency Analyser Type 2131. The resultant data file, covering third-octave bands from, say, 10 Hz to 8 kHz is subtracted from a corresponding data file obtained by identical hardware-analysis of the target time history. This difference file forms the basis for the (first) error-correction file.

Then follow two processes, broadly effecting analysis of the error, then synthesis of a compensated time history that will replace the original aircraft recording.

In the analysis module, the target time history (stored on disc) is applied to a recursive digital filter and decomposed into its 'component band-files' - this is a Fourier-like process in the time domain producing one-third octave-wide files.

The component band-files (which may be numerous) are stored on disc pending synthesis by a complementary module. This produces a modified time history comprising the sum of the component band-files weighted by coefficients that are derived from the values in the error correction file.

At the end of the process, a new time history file will exist that contains all the constituent frequency components of the target file, but these being differentially weighted, a different noise field will be produced on playing the new file into the chamber.

If the resultant new (*ie* second) error spectrum is not sufficiently small it may be used to produce a further weighted sum of component band-files via a repeat application of the synthesis module, and so on. However, small differences in chamber topography, amplifier gains etc impose an early limit to the number of iterations.

Existing procedures in the laboratory enable data to be acquired at a high sampling rate (32 kHz) and written out to 300 mB disc storage. Other procedures allow disc data to be put out at this rate into a high-power sound reproduction system. Fig 2 shows in principle the mechanisation of the whole package.

2.2 Analysis by digital filter

2.2.1 General

The process of filtering the target waveform is thus fundamental to the method. The filter used is effectively a Butterworth (maximally flat) 4th-order bandpass filter with zero phase shift, implemented on the Array Processor (AP) and windowed so that no discontinuities are introduced although only a small portion of the whole time history can be accommodated for processing at any one time in the AP.

Rather than merely define the filter in terms of a difference equation, or alternatively as a z-plane transfer function, it has been thought worthwhile to outline the derivation of these expressions in Appendix B, which itself seemed to necessitate Appendix A, where an outline is given of some relevant features of s-plane and z-plane analyses.

The solution to a difference equation having the form of equation (B-9) was conveniently already existing as a module in the APMATH library of the Array Processor. As shown in Appendix B, the band-pass filter derives from a first-order lag transfer function.

After passing forwards through the filter, the data is time-reversed for a second pass which cancels the phase shift introduced on the first pass[1], while providing steeper attenuation characteristics in the stop bands. The forward/reverse passes are then repeated for further selectivitiy.

As the object of the process is finally to synthesize a revised time history without added discontinuities, only the central portions of each data set being filtered are in fact retained. To elaborate: storage in the AP allows 32K data points (*ie* representing 1 second of time history) to be processed at one time, allowing for the necessary location shifts in memory during manipulation of the data. The 32K *data points are first windowed* by cosine tapering to zero of the first and last 4K points, and then only the central 16K data points are retained as a ½ second output component band-file. Thus n seconds of target file time history produce (2n - 1) component band-files each ½ second long.

As the data passes repeatedly through it, the filter has its third-octave pass band centred sequentially on the standard ISO centre frequencies, to be compatible with the B/K 2131 for hardware analysis: hence for decomposition into m 1/3-octave bands, there will be produced m(2n - 1) ½-second files, stored on disc. Clearly, this must be a time-consuming process.

2.2.2 Performance

The attenuation/frequency characteristic of the filter will now be discussed briefly. In fact, it is preferable to speak of the aforesaid characteristic as pertaining to the process, rather than to the filter, because as has been seen, the output of the process is a summed function of individual filter outputs. Thus instead of exciting a single filter by stepping through a succession of sinusoids and plotting the output attenuation in one band, a more valid result is obtained by plotting the simultaneous output of all filters, for one forcing sinusoid.

Accordingly, Fig 3a shows the response to a single (*ie* FWD + REV) pass through the process for a 1 kHz input. It is seen that the skirts of the filter response fall off at about -12 dB/octave, but the initial rate is about -33dB/octave. The first figure is compatible with the -6 dB/octave characteristic expected from each pass through the filter (*ie* FWD), remembering that the second (REV) pass multiplies the attenuations and produces a further -6 dB in the final result. It is not known why the initial rate of attenuation is as high as has been observed above. Fig 3b shows the overall characteristic when a double pass (*ie* 2 × (FWD + REV)) is used. As expected, the logarithmic slopes are doubled.

2.3 Synthesis

Conceptually, this is simply the concatenation of all the ½ second component band-files already stored on disc, and a summation over all bands to produce the final output file. In fact, the data is handled again by the AP, in ½-second slices - the required weighting factors are applied and a sequence of multiply-and-add operations builds up in the AP a composite ½-second file with weighted contributions from all its component band-files. This ½-second output file is then sent back to be concatenated on disc with its immediate predecessor in time. Thus the length of the final output file is (2n - 1)/2 seconds, *ie* half a second shorter than the original target time history.

A special case of the output file is that where the weightings are unity - when a file whose characteristics match that of the original target file should be produced. Fig 4a shows a portion of a time history of a helicopter noise field, and Fig 4b&c the reconstruction by such unit weighting for single and double complete passes respectively. It should be noted that because of undesired but unavoidable attenuation in the pass band of the filter, the frequency components present in the target file (which are unlikely to lie at exact band-centre) have amplitude errors which result in the reconstructed waveforms

not precisely imaging the original. For this reason, the waveforms of Fig 4 do not have identical y-axis scales and these are omitted from the plots, which are intended to be of a qualitative nature. It has in fact been found to improve the iteration process if the first correction file produced, to be used in producing the first iterated synthetic output file, is actually derived via this 'unity-reconstructed' file and not the true target file (which of course still provides the ultimate error spectrum to be minimised).

2.4 Correction file

It should be mentioned that before the laboratory computer system was modified to include on-line hardware spectral measurement and data storage via the B/K 2131, considerable effort was put into developing off-line routines that would accept narrow-band (1 Hz) spectral data via FFT programs in order to produce 1/3-octave data to be used in the derivation of correction files. The process clearly adds even more time to that already needed, and it was necessary to model the 1/3-octave band filters in the B/K equipment fairly closely, because in the final analysis, a verdict on the goodness of the compensation was still made via on-line measurement using the B/K 2131. As stated, the software 1/3-octave routine proved unnecessary in the end.

Other approaches to the optimisation problem have been tried with little success, that is, by using more complicated algorithms to derive a correction file, rather than merely getting weighting factors from the error file. The difficulty is that the decomposition process of section 2.2.1 is obviously far from perfect in both pass and stop bands, and it was not found possible to reduce errors to acceptably small limits by making use of the estimated imperfections in the filtering process. As already stated, repeated derivation of error files and their application as correction coefficients has been found to be the only way to achieve the improvements noted (*eg* Fig 1).

2.5 Postcript

A revised *modus operandi* has been developed since the main text was written, and brief notes are given here.

It has always been appreciated that there was a problem in dealing with the lower frequency bands that are of especial interest in handling helicopter noise. For example, at a centre frequency of 20 Hz the 1/3-octave bandwidth is about ±2.5 Hz: the effective truncation of analysis time to 1 second means that even after the retention of only the centre half second and use of tapering, the transient (impulse) response of the filter to the too-short section of time history can be recognised.

At the same time, difficulties were being met in trying to implement alternative filters of higher order. Round-off computational errors have traditionally restricted the filter order to one or two, but here it was found that as the centre frequency and bandwidth decreased, the second-order solution became increasingly erroneous and finally unstable for centre frequencies typically around 50 Hz. Double precision arithmetic had already been used as far as possible when it was realised that the use of the AP in the analysis module was the cause of the trouble. Although the AP word-length is greater than the single precision word-length on the PDP 11/84, it is much shorter than the double precision word-length; thus in effect accuracy was being sacrificed to speed.

Accordingly, the program has been reconfigured for double precision working completely on the PDP 11/84, with the very considerable advantage that there is no longer any need to analyse in steps of 1 second - it becomes a continuous process over the whole duration of the input time history. The AP is only (and very advantageously) used in the synthesis module where, as before, it functions as an accumulator, but this time the process is considerably speeded up, because the amount of file manipulation on disc is reduced. The overall time for analysis and synthesis is of the same order as originally.

3 CONCLUSIONS

A digital method has been demonstrated for analysing a target signal field and synthesizing another one related to it. The method is simplistic, lengthy and approximate, but has been successfully mechanised. Significant improvements have been observed in the reproduction of aircraft cabin noise fields.

It is expected that further work will be carried out using digital bandpass filters with different frequency characteristics with a view to effecting optimum performance.

Acknowledgment

The author wishes to acknowledge with gratitude the considerable efforts of Dr J.A. Chillery in developing the real-time computer system that has been built up in FS(F)4 at RAE[2], and his many contributions to the overall strategy of the work covered by this Memorandum.

Appendix A

GENERAL THEORY

The s-plane (complex frequency) has long been deemed to be of more utility than the (real) time plane as an aid to the design and analysis of Continuous Control Systems (in the widest interpretation of their definition).

The Laplace Transform $F(s)$ of a time function $f(t)$ allows direct access to the convenient representation of modal characteristics and system responses on the s-plane. The alternative manipulation of $f(t)$ using convolution is in general more difficult and less informative.

When sampled-data (*ie* digital) systems are considered, a continuous time-signal $f(t)$, sampled every T seconds, is represented by $f^*(t)$. The latter has a Laplace Transform $F^*(s)$ that contains non-algebraic factors $\exp(-nsT)$ for $n = 0,1,2,\ldots$ and is not very tractable in this form.

A convenient transformation of

$$z = \exp(sT) \qquad \text{(A-1a)}$$

then enables the Laplace Transform to be written in terms of z, when it is known as the z-Transform. In this form the awkward factors referred to above become

$$z^{-n} \qquad \text{for} \qquad n = 0,1,2,\ldots$$

and they can be interpreted as Delay operators in the transformed time series, *ie*

$$F(z) = e(0) + e(T)z^{-1} + e(2T)z^{-2} + e(3T)z^{-3} + \ldots \ .$$

This method of describing the sampled time series $f^*(t)$ in terms of the delay operator z^{-1} is very powerful, enabling transfer functions of discrete processes to be expressed as rational functions, and difference equations to be derived from them, giving the current output value $y(i)$ as a sum of past output values $y(j)$ for $j = i-1, i-2,\ldots$ and present and past input values $x(k)$ for $k = i, i-1, i-2, \ldots$. This will be done in Appendix B for the filter under discussion.

However, it will be realised that the above definition of z in equation (A-1a) implies the inverse relation

$$s = \left(\frac{1}{T}\right) \log_e(z) \qquad \text{(A-1b)}$$

and if the digital equivalent $H(z)$ to a continuous transfer function $H(s)$ is sought, then some approximation to the logarithm must be used. A well-known

approximation leads to equation (A-1c) in the next section, but first there follows a brief introduction to some graphical techniques.

A.1 Mappings

The fundamental feature of sampled data is that unless a continuous time series is band-limited to below the Nyquist frequency $f_N = f_s/2 = (1/2T\ Hz)$, then no longer can the process be uniquely inverted to reproduce the original waveform. This mechanism (aliasing) occurs because of the duality existing through the Fourier Transform between the processes of multiplication and convolution in the time and frequency planes.

Thus, because a time series is in effect a sequence of products of unit delta function pulses and a continuous time history (Fig A1) then in the frequency plane the resultant convolution is seen to be periodic with repetitions of the spectrum at intervals of f_s (see Ref 3).

Hence in Fig A1 the part of the spectrum containing genuine information is the Base-band from $-f_s/2$ to $+f_s/2$ and clearly this will be corrupted by spurious folding-down of frequencies from higher bands unless the above-mentioned band limiting is assured.

Looking at the (discrete) s-plane, it is seen that the area of interest is confined to the strip between $s = j\omega_s/2$ and $s = -j\omega_s/2$. Any poles or zeros appearing in this region (Fig A2) will, by virtue of the periodicity noted in Fig A1, also appear in all other complementary strips.

As the imaginary axis forms the boundary between stable and unstable modes of system behaviour, design attention in the discrete s-plane is focussed on the so-called Primary Strip in Fig A2.

Recalling the transformation $z = \exp(sT)$ it can be shown readily by substituting $s = \sigma + j\omega$ that the primary strip maps into a circle on the z-plane, see Fig A3a. The radius of the circle is unity and the mappings of a single pole and a pair of complex poles is also shown in Fig A3a for clarity. It is seen that poles outside the unit circle will result in unstable modes.

As stated in the preceding section, much design experience in the field of continuous (analogue) filters can be made use of by an approximation to the z-transform, which is equivalent to mapping the unit circle on the z-plane to a new plane. Different authors have used different forms of this transformation with the result that their terminologies and illustrative diagrams can cause confusion.

Essentially, the transformation is the bilinear relation

$$w_1 = u_1 + jv_1 = \frac{z - 1}{z + 1} \qquad \left(z = \frac{w_1 + 1}{w_1 - 1}\right) . \tag{A-1c}$$

This mapping projects the unit circle on the z-plane into the entire LH w_1-plane (Fig A3b). It can be seen that traversing the unit z-circle from (1) to (2) corresponds to the whole axis of positive frequencies on the new plane. If, therefore, a mapping is required between the entire LH continuous w_1-plane and the primary strip of the discrete s-plane (Fig A3a), via the z-plane, then the relation between the corresponding frequencies must be highly nonlinear, or warped.

Three variants of the bilinear transformation are commonly found and will be illustrated briefly.

(1) This is the basic form already introduced above in equation A-1c). From this and the definition $z = \exp(sT)$ we can derive the relation

$$w_1 = \tanh(sT/2) . \tag{A-2a}$$

Then by setting $w_1 = jv_1$ and $s = j\omega$ we get the warping equation

$$v_1 = \tan(\omega T/2) \tag{A-2b}$$

which links a given frequency in the discrete s-plane to some other frequency on the continuous w_1-plane.

This important curve is shown in Fig A4a (see Ref 4).

(2) Correct dimensionalising and normalisation with respect to the sampling frequency is introduced by the factored mapping

$$w_2 = \frac{2(z - 1)}{T(z + 1)} \tag{A-3}$$

which leads to the corresponding expression

$$w_2 = \frac{2}{T} \tanh(sT/2) \tag{A-4a}$$

and frequency mapping

$$v_2 = \frac{2}{T} \tan(\omega T/2) . \tag{A-4b}$$

This is shown in Fig A4b, drawn to illustrate the relation between frequency ratios, as can be found in the literature[5]. Also shown is the line defining

$$v_2 = \omega .$$

This is equivalent to using the bilinear transform with immediate substitution of continuous-plane parameters, and is seen to be a reasonable approximation to the tangent function up to, say, $\omega T = 1$. Beyond this, frequency warping becomes significant and the modified continuous-plane frequencies should be used.

It is important to realize that equation (A-3) is an exact relation, having certain properties, desirable or otherwise, but is only an approximation to the exact inverse of $z = \exp(sT)$ viz:

$$s = \frac{1}{T} \log_e(z) \quad .$$

The right-hand-side of equation (A-3) is in fact the first term in an approximation to $\log_e(z)$ as was mentioned in equation (A-1), or, equivalently, derived by similarly truncating $\exp(sT)$, *ie* $\exp(sT/2)/\exp(-sT/2)$.

Yet another way of visualising equation (A-3) as being an approximation is by considering the operation (1/s) - integration in the complex plane - and its counterpart in the time domain.

Fig A5 shows that when

$$y = \int x dt$$

is evaluated by trapezoidal approximation, the current estimate of y (*ie* y_n) is given by

$$y_n = y_{n-1} + \frac{T}{2}(x_n + x_{n-1})$$

or, recognizing z^{-1} as the unit delay operator,

$$Y(z) = Y(z)z^{-1} + \frac{T}{2} X(z)z + \frac{T}{2} X(z)z^{-1}$$

which gives the z-transfer function as

$$\frac{Y(z)}{X(z)} = \frac{T(1 + z^{-1})}{2(1 - z^{-1})} \quad . \qquad \text{(A-5)}$$

This expression, describing the operator (1/s) , is seen to be correctly the reciprocal of the relation already given in equation (A-3) for the operator (s) .

If the filter is being designed on the z-plane with, say, cut-off frequency ω_{dc} , the substitution of ω_2 by relation equation (A-3) will produce a continuous-plane approximation where the cut-off frequency of the equivalent continuous filter is at a frequency ω_{ac} . Thus we could have, for example, the mapping as sketched in Fig A4c, enabling ω_{ac} to be read off against a known ω_{dc} .

(3) A further development of (1) is the transform

$$w_3 = K\frac{z-1}{z+1} ,$$

where $K = \dfrac{\Omega_{co}}{\tan(\omega_c T/2)}$,

where Ω_{co} is a (cut-off) frequency on the continuous plane for which there is some *a priori* reason for mapping to a specific similar point on the discrete plane - generally because tables may exist for the design of a particular analogue filter. For generality we retain the parameter Ω_{co} but usually it may be equated to unity.

Then, the constant K (which does not affect the shape of the mapping) ensures a convenient system of scales for the graphs. Thus

$$v_3 = \mathrm{Im}(\omega_3) = \frac{\Omega_{co}}{\tan \omega_c T/2} \tan \frac{\omega T}{2}$$

as shown in Fig A4d (see Ref 6).

Appendix B

DERIVATION OF BAND-PASS FILTER USED

B.1 General

It has been shown above that methods exist whereby the continuous s-plane may be mapped to the discrete z-plane. In particular, we must now derive a z-transfer function for a band-pass digital filter, so that it may be implemented on the AP.

The steps in the process will be:

(1) to effect a mapping on the continuous plane between a prototype low-pass filter and a general band-pass filter.

(2) To extend this mapping into the z-plane by obtaining an approximate relation between s and z that will map the prototype low-pass filter into a digital band-pass filter, without determining its numerical parameters.

(3) To obtain such parameters by substitution of $z = \exp(sT)$ into the relation found in (1) above.

(4) To obtain the z-transfer function by substituting these numerical values in (2) above and thence write down the difference equation.

B.2 Details

(1) Guillemin has shown[7] that other more complicated continuous-plane filters may be mapped by frequency transformations from the low-pass form which is regarded as a prototype. (This preparatory mapping solely in the s-plane is not to be confused with s- to z-plane mappings considered above.)
Take the prototype

$$P(\lambda) = \frac{1}{1 + (\lambda/\Omega_{co})} , \qquad (B-1)$$

where $\lambda = \sigma_B + j\omega_B$

and Ω_{co} is the cut-off frequency.
(This nomenclature is chosen arbitrarily to allow the familiar complex variable $s = \sigma + j\omega$ to be used as the output variable.)

We require the new variable s to be such that given $P(\lambda)$ as in equation (B-1) above, then $P(s)$ will describe a band-pass function. Values of λ in equation (B-1) are next mapped, noting that in the λ-plane

$\lambda = 0$ gives the centre of the (low) pass band,

$\lambda = \infty$ gives the high-frequency asymptotic behaviour.

In the s-plane, we need $\lambda = 0$ to be mapped to a pair of points on the frequency axis (the band-pass centre frequency $j\omega_0$ and its conjugate), and $\lambda = \infty$ to map to $s = 0$ and $s = \infty$ for attenuation at low and high frequencies. These conditions are equivalent to specifying complex zeroes at $\pm j\omega_0$ and a simple pole at the origin of the s-plane viz:

$$\lambda = \frac{s^2 + \omega_0^2}{cs} \quad . \tag{B-2a}$$

Thus, having defined s implicitly in terms of λ, as was required, we next find the relation between their imaginary parts by putting $s = j\omega$ in equation (B-2a) and equating $\mathrm{Im}(\lambda)$ to ω_B from equation (B-1), giving

$$\omega_B = \frac{\omega^2 - \omega_0^2}{c\omega}$$

or

$$\omega^2 - c\omega_B\omega - \omega_0^2 = 0 \quad . \tag{B-2b}$$

Equation (B-2b) may now be used to obtain the two s-plane values corresponding to the λ-plane cut-off frequency Ω_{co} in equation (B-1). Fig A6 is the graphical expression of equation (B-2b) and is a convenient way of deriving its roots. From it can be seen that the values of ω for $\omega_B = \Omega_{co}$ are ω_u and $-\omega_\ell$, where ω_u and ω_ℓ are the -3 dB values for the band-pass filter. Then elementary theory of equations gives the values of the sum and product of these roots as

$$\omega_u - \omega_\ell = c\Omega_{co} \tag{B-2c}$$

and

$$\omega_u\omega_\ell = \omega_0^2 \quad . \tag{B-2d}$$

From equation (B-2c), for the case of filters normalised to $\Omega_{co} = 1$ rad/s, we get

$$c = \omega_u - \omega_\ell$$

and hence

$$\lambda = \frac{s^2 + \omega_u\omega_\ell}{s(\omega_u - \omega_\ell)}$$

but generally we may write equation (B-2a) as

$$\lambda = \Omega_{co}\,\frac{s^2 + \omega_u\omega_\ell}{s(\omega_u - \omega_\ell)} \quad . \tag{B-3a}$$

[In passing, we note that by substituting equation (B-3a) into equation (B-1) we obtain the s-plane transfer function of the band-pass filter in terms of ω_u and ω_ℓ, viz

$$\frac{s(\omega_u - \omega_\ell)}{s^2 + s(\omega_u - \omega_\ell) + \omega_u\omega_\ell} \quad . \tag{B-3b}$$

Fig A7 shows the familiar shape of the transfer function of equation (B-3b); however, it is equation (B-3a), the frequency transformation function, that will be used in the next section.]

(2) The mapping of the prototype low-pass filter (λ-plane) onto the z-plane is via the s-plane using equation (B-3a). Thus, using the bilinear transform by putting $s = k(z-1)/(z+1)$ in equation B-3a) we get

$$\lambda = B\,\frac{(z^{-2} - 2Az^{-1} + 1}{1 - z^{-2}} \quad , \tag{B-4}$$

where $B = \Omega_{co}\,\dfrac{(k^2 + \omega_p)}{k\omega_d}$, using the nomenclature $\omega_p = \omega_u\omega_\ell$

$\omega_d = \omega_u - \omega_\ell$

and $A = \dfrac{k^2 - \omega_p}{k^2 + \omega_p}$.

(Note that k is still undetermined, and, in fact, as the coefficients A and B are those actually required, k will never be found explicitly.)

This expression for λ is now substituted into the prototype equation (B-1) to give

$$\frac{Y(z)}{X(z)} = \frac{\frac{1}{B} - \left(\frac{1}{B}\right)z^{-2}}{\left(1 - \left(\frac{1}{B}\right)\right)z^{-2} - 2Az^{-1} + \left(\frac{1}{B}\right) + 1} \quad . \tag{B-5}$$

(3) To determine the constants A and B in section (2) above, we next substitute for powers of z^{-1} in equation (B-4) remembering that for points on the unit circle on the z-plane we have

$$z^{-1} = \exp(j\omega T) = \cos(\omega T) - j\,\sin(\omega T) \quad .$$

Some algebra then reduces the right-hand side of equation (B-4) to

$$\frac{jB(A - \cos(\omega T)}{\sin(\omega T)} \quad . \tag{B-6}$$

This maps to the general continuous frequency $\omega_B = \mathrm{Im}(\lambda)$, and we proceed with the mapping of other frequencies thus:

when

$$\lambda = 0 \quad \text{(mapping to band-pass centre-frequency)}$$

we get

$$A = \cos(\omega T) \quad ,$$

ie

$$\omega_{00} = \frac{1}{T} \cos^{-1} A \quad .$$

To use the mapping at the -3 dB points, referring back to Fig A6 we put $\mathrm{Im}(\lambda) = \omega_B = -\Omega_{co}$ and $+\Omega_{co}$ successively, thus:

$$-\Omega_{co} = \frac{B(A - \cos(\omega_\ell T))}{\sin(\omega_\ell T)}$$

and

$$+\Omega_{co} = \frac{B(A - \cos(\omega_u T))}{\sin(\omega_u T)} \quad .$$

From these equations we get the following relations - by division

$$A = \frac{\cos\left[(\omega_u + \omega_\ell)\frac{T}{2}\right]}{\cos\left[(\omega_u - \omega_\ell)\frac{T}{2}\right]} \quad . \qquad \text{(B-7)}$$

By subtraction

$$B = \frac{\Omega_{co}}{\tan\left[(\omega_u - \omega_\ell)\frac{T}{2}\right]} \quad . \qquad \text{(B-8)}$$

Thus the coefficients in equation (B-5) may now be calculated to enable the final difference equation to be written down. (Ω_{co} is arbitrary and for convenience is set equal to 1 rad/s.)

(4) Using the delay property (shifting theorem) of the bilinear transform on equation (B-5) gives the time domain solution

$$\left(1 + \frac{1}{B}\right)y_i(t) - 2Ay_{i-1}(t) + \left(1 - \frac{1}{B}\right)y_{i-2}(t) = \left(\frac{1}{B}\right)x_i(t) - \left(\frac{1}{B}\right)x_{i-2}(t)$$

or

$$y_i(t) = \frac{1}{(1 + B)}x_i(t) - \frac{1}{(1 + B)}x_{i-2}(t) + \frac{2AB}{(1 + B)}y_{i-1}(t) + \frac{(1 - B)}{(1 + B)}y_{i-2}(t) \quad . \qquad \text{(B-9)}$$

This is the equation which is implemented on the Array Processor after the coefficients have been inserted from equations (B-7) and (B-8).

It is to be noted that the relation of equations (B-4) and (B-6) is shown plotted in Fig A8. This is the warped relation between frequencies on the continuous plane for the prototype lowpass filter and those on the discrete plane for the bandpass filter. This agrees well with Fig 3a which was shown for a forward pass followed by a reverse pass.

Appendix C

ITERATION PROCESS (SYSTEM-SPECIFIC DETAILS)

For local convenience, there follow working notes on the procedures that must be followed to go through an iteration. It is assumed that a good quality tape recording exists (preferably in PCM format to retain maximum S/N ratio, together with the system hardware as outlined in Fig 2).

A data analysis package 'DATS' (Prosig Ltd) is present on the system and its modules and facilities have been used extensively in the work. The procedure 'TESTX4' that puts out disc data in real time to the analogue power amplifiers is part of a suite of programs developed by Signal Computing Ltd.

(1) Acquire onto 300mB disc a suitable recording of target noise using PCM recorder and DATS/ACQUIR .

(2) Use DATS/ARITH to scale the numbers in (1) to a level suitable for subsequent output via the A/D convertor to the power amplifiers.

(3) Obtain the 1/3 oct. spectrum of the O/P file in (2) using B/K Type 2131 Analyser. Use /AC2131 to acquire this data onto disc file.

(4) Run LASSEX (a DATS-type JOB that calls the digital filter module /LASSTP) on the target noise time history obtained in (2).

(5) Use /XASCOM (the synthesis module) on O/P of (4), with a unity-gain Correction file. This produces the synthetic target file.

(6) Output this into the chamber using 'TESTX4', while simultaneously obtaining the 1/3 oct. data for the actual chamber noise as in (3) above.

(7) Obtain error (difference) file from (3) to (6) by DATS/ARITH and then run /DIFFER to get a 1st Correction file.

(8) Use /XASCOM on component-band files found in (4), this time with the 1st Correction file. The O/P from this operation is the 1st Compensated output file.

(9) Repeat (6) and (7) above to examine the improvement in error spectrum and to proceed to a further iteration if necessary by repeating (8), using the new (2nd) Correction file.

REFERENCES

No.	Author	Title, etc
1	R.W. Hamming	Digital filters. Prentice-Hall (1977)
2	J.A. Chillery J.B. Collister	A practical helicopter cabin noise simulator. Paper presented at the Second IEE International Conference on simulators. University of Warwick, Coventry, UK, September 1986
3	E.O. Brigham	The Fast Fourier Transform. Prentice-Hall (1974)
4	R. Saucedo E.E. Schiring	Introduction to Continuous and Digital Control Systems. Macmillan (1968)
5	S.M. Bozic	Digital and Kalman filtering. Arnold (1979)
6	R.E. Bogner A.G. Constantinides	Introduction to digital filtering. Wiley (1975)
7	E. Guillemin	Synthesis of passive networks. Wiley (1957)

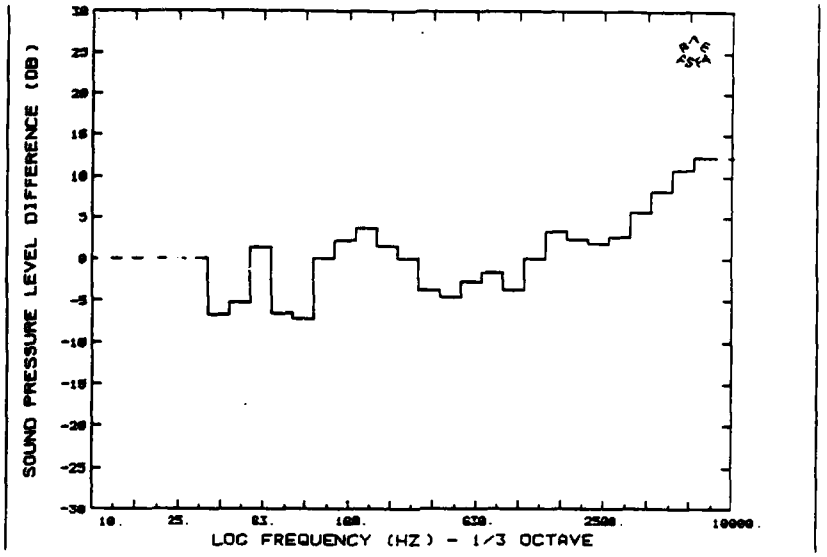

Fig 1a

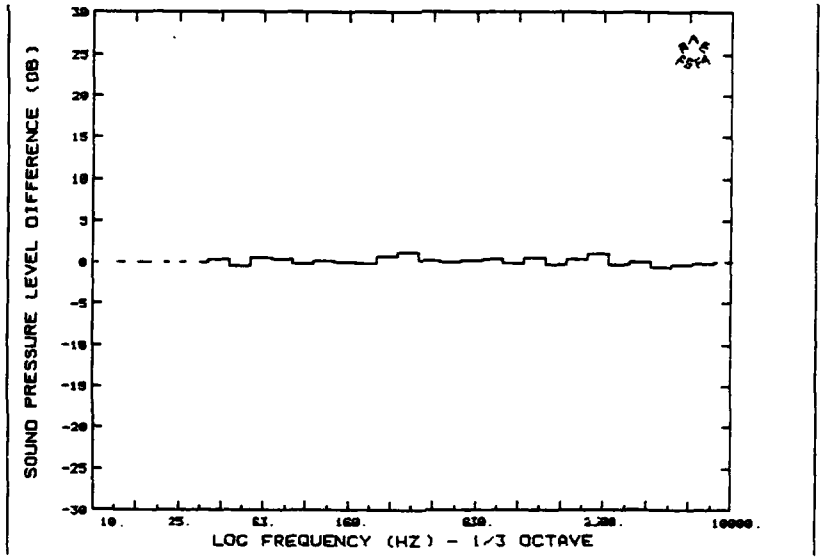

Fig 1b

Fig 1a&b Third-octave error spectra (jet aircraft)
(a) original (b) improved

Fig 1c&d

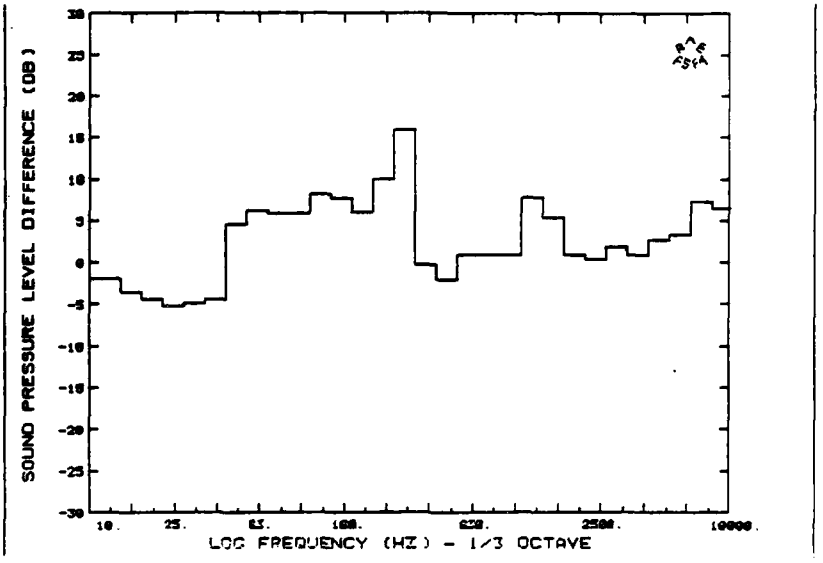

Fig 1c

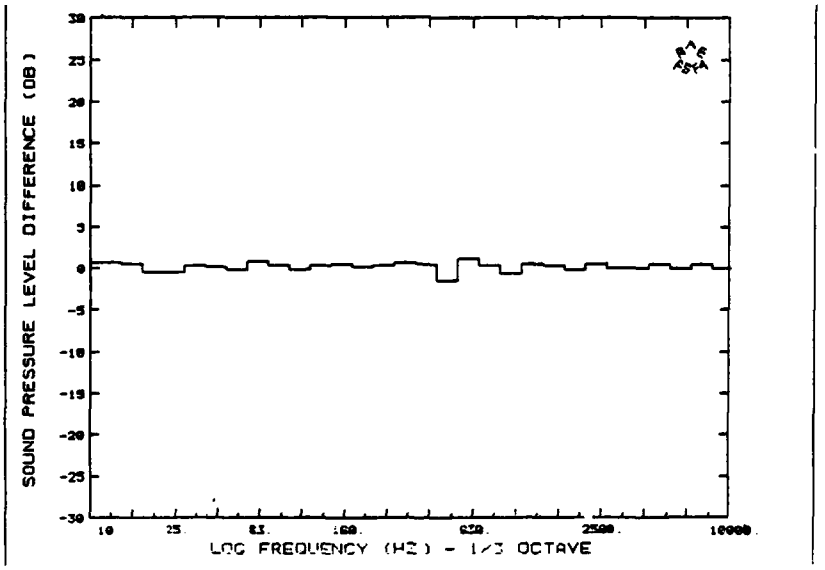

Fig 1d

Fig 1c&d Third-octave error spectra (helicopter)

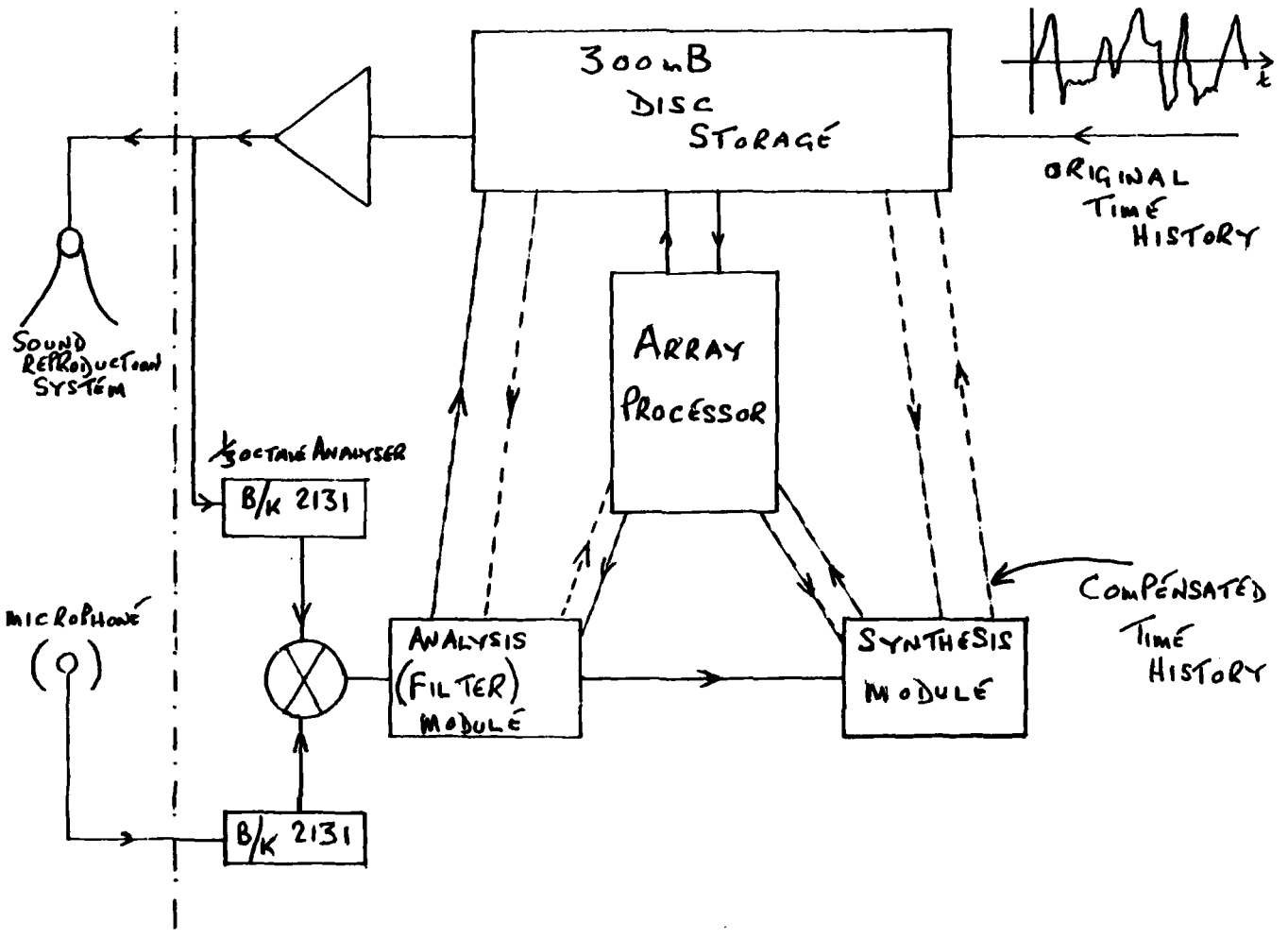

Fig 2 Implementation of compensation process

Fig 2

Fig 3a&b

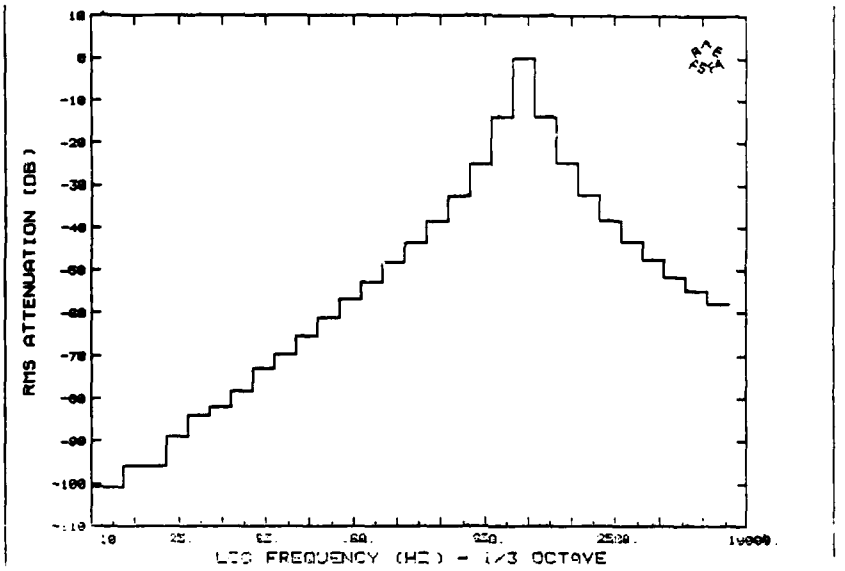

Fig 3a Single complete pass (ie FWD + REV)

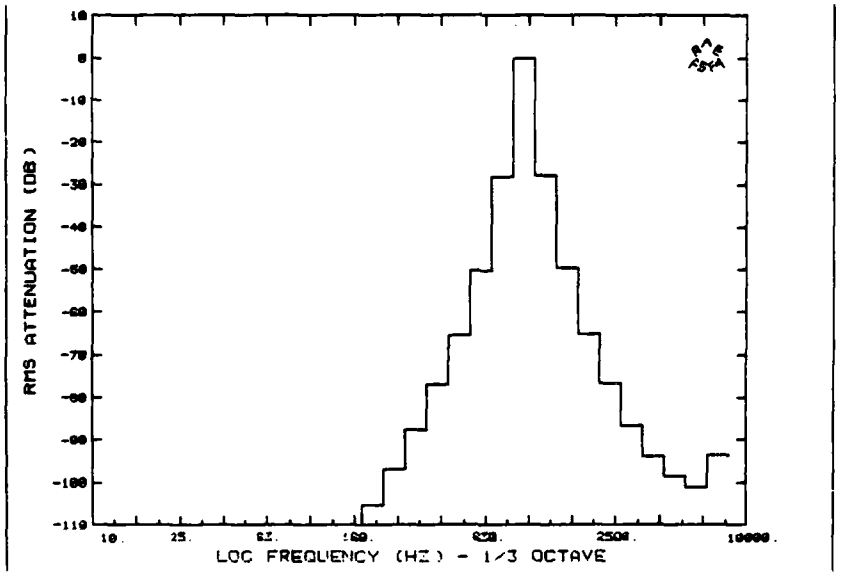

Fig 3b Double complete pass

Fig 3 Frequency characteristic of digital filter process

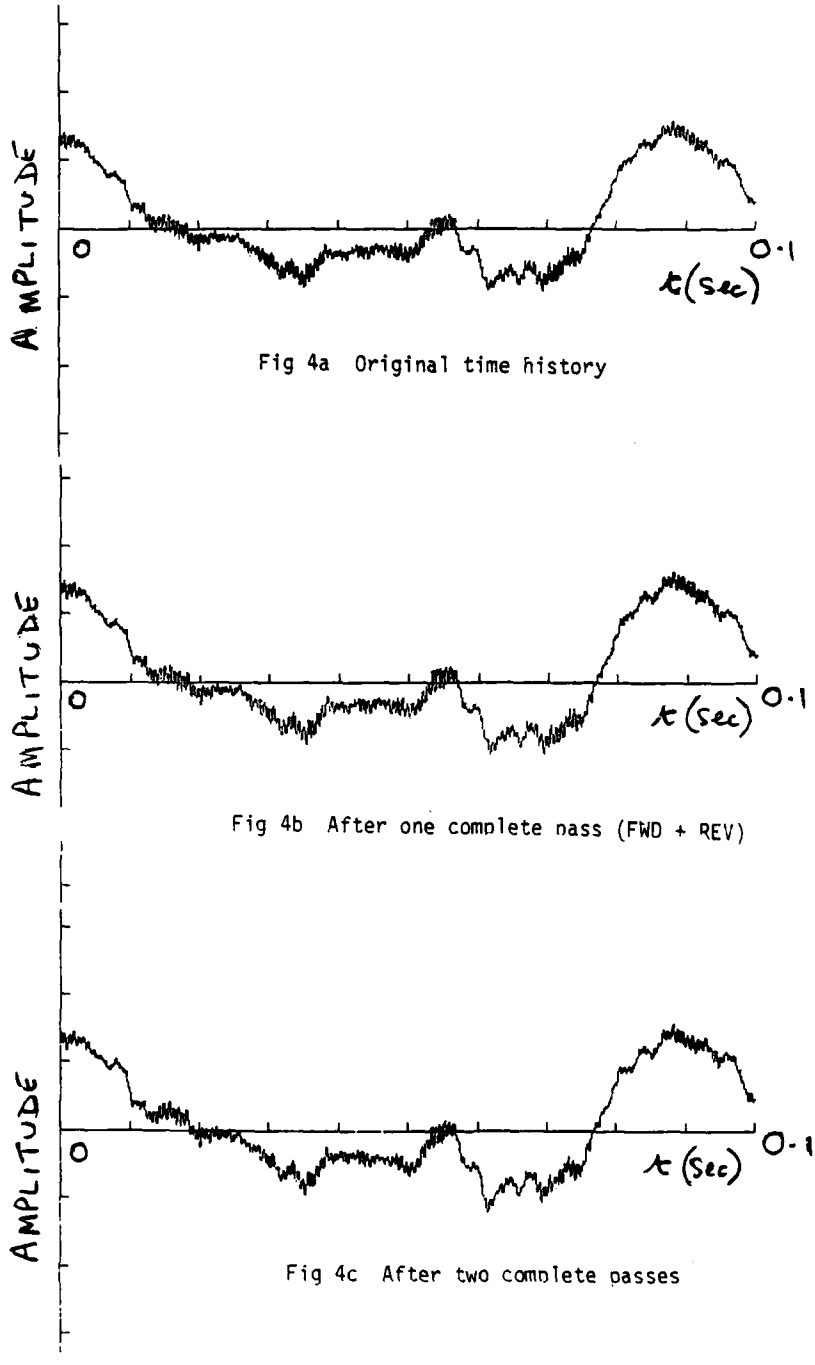

Fig 4a Original time history

Fig 4b After one complete pass (FWD + REV)

Fig 4c After two complete passes

Fig 4 Reconstruction of original time history by use of unity correction file (y-scales differ - see section 3)

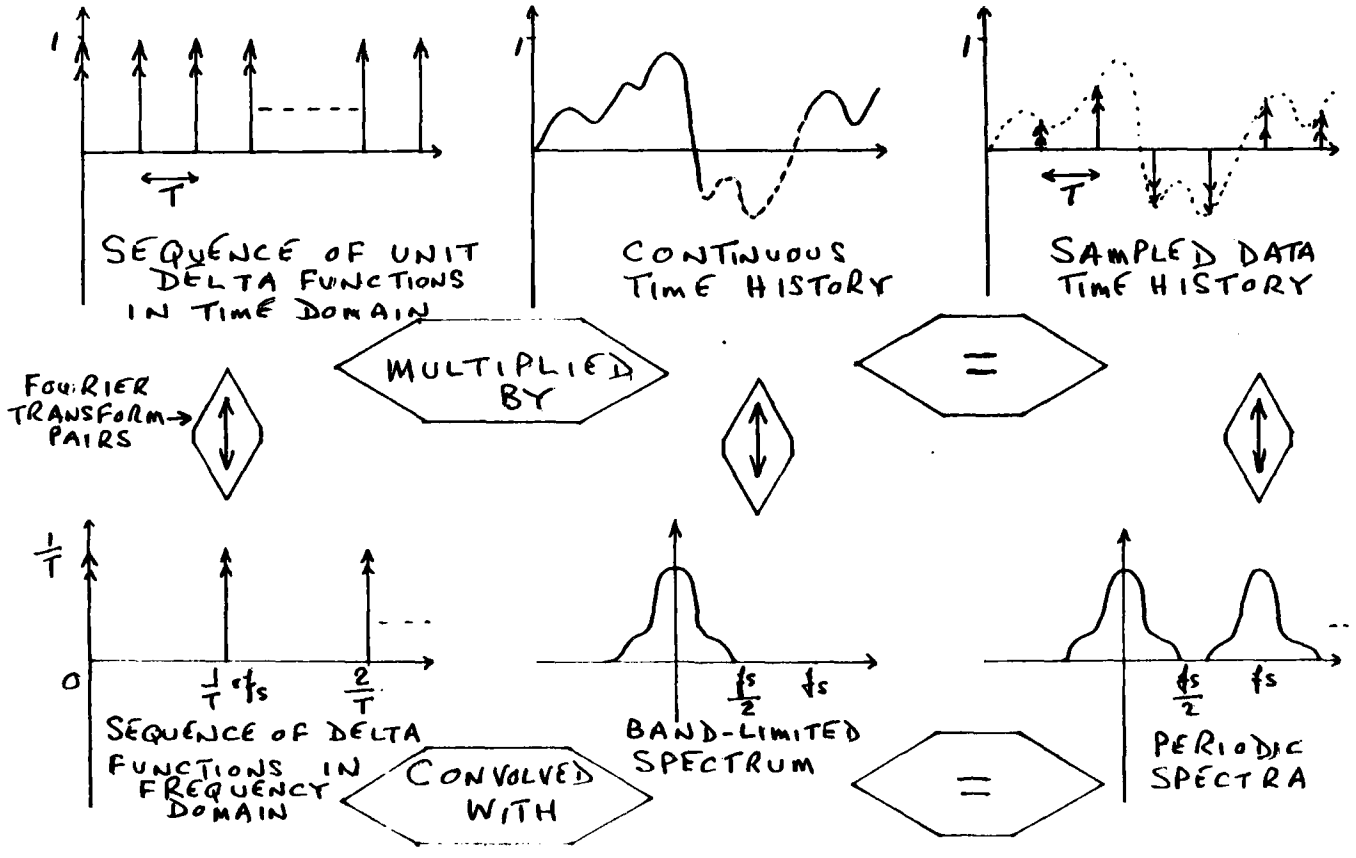

Fig A1 Periodic spectra produced by sampling in time (no aliasing)

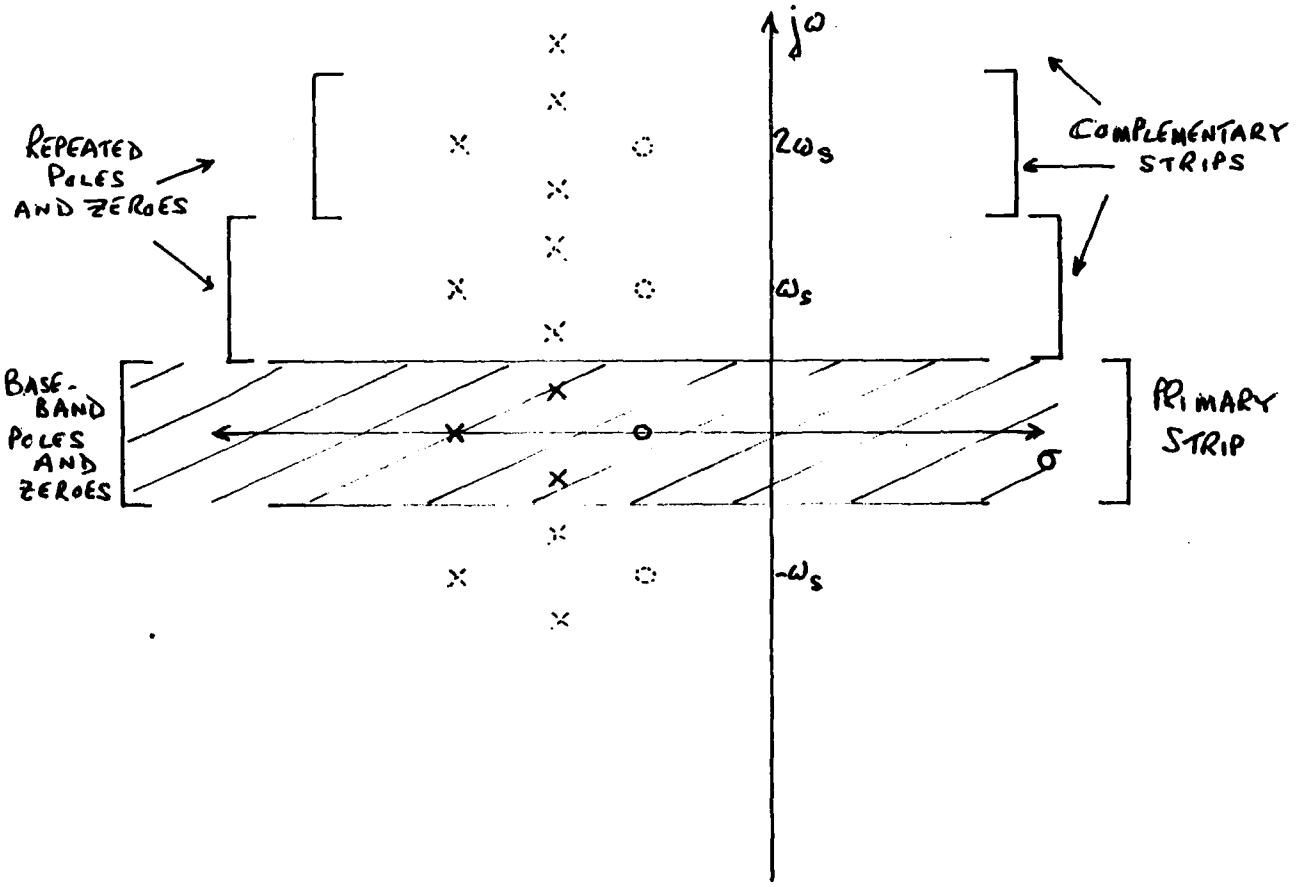

Fig A2

Fig A2 The discrete s-plane primary strip and its images

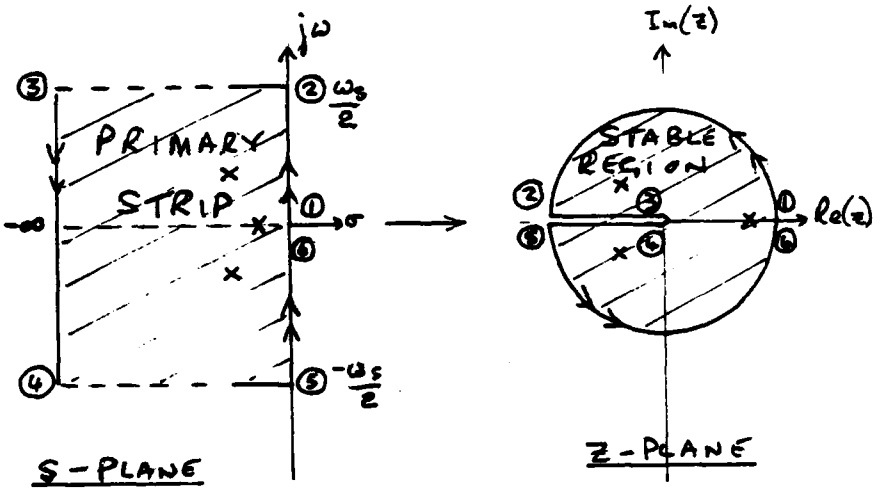

Fig A3a Mapping of s-plane to z-plane

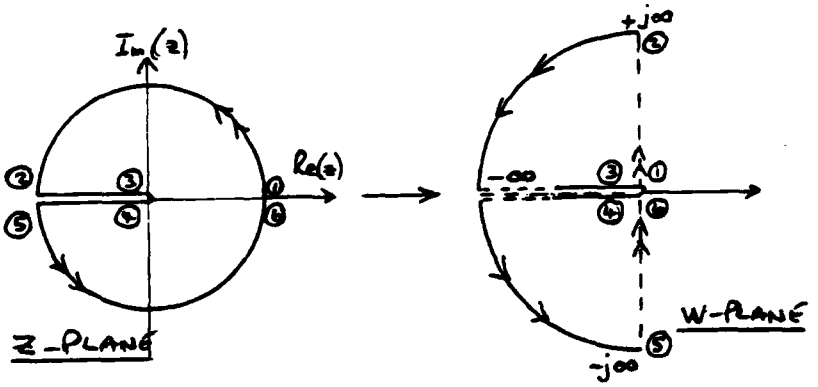

Fig A3b Mapping of z-plane to w-plane

Fig A4a&b

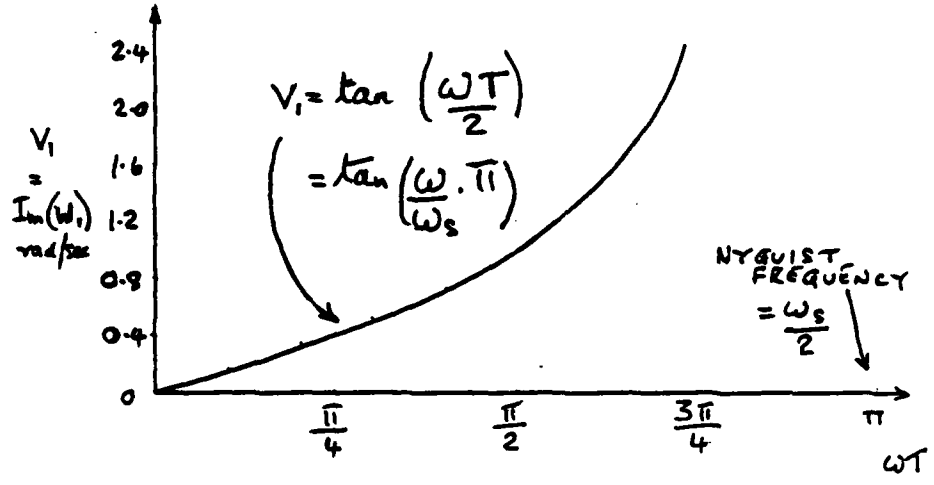

Fig A4a Warped frequencies (s-w_1 planes)

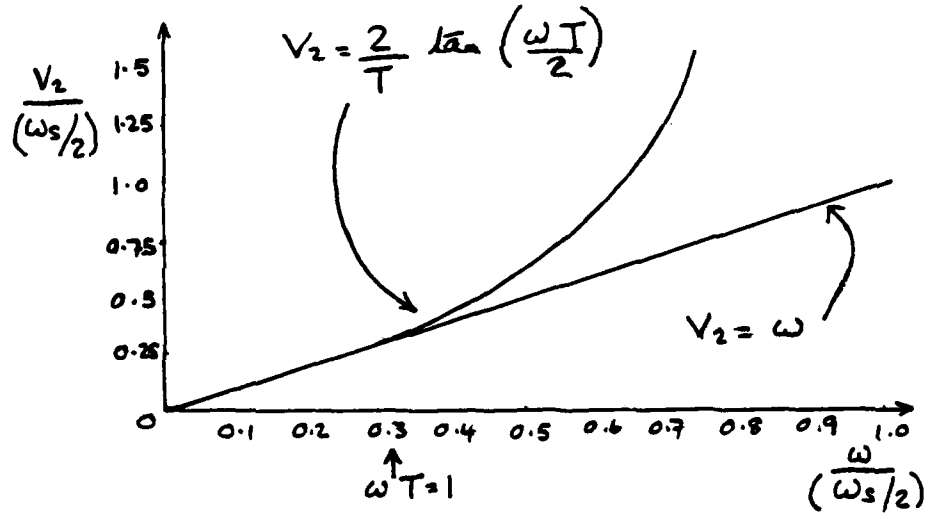

Fig A4b Warped frequency ratios (s-w_2 planes)

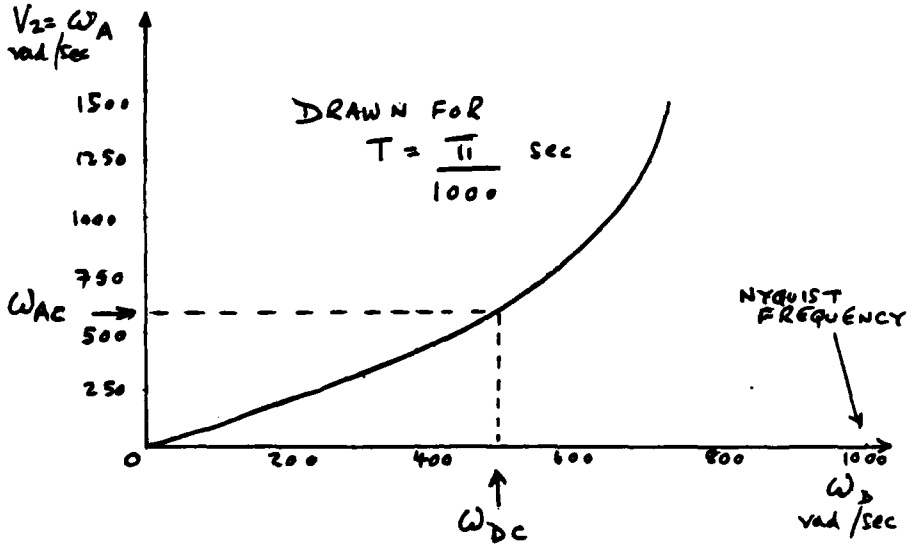

Fig A4c Example of warped frequencies (s-w_2 planes)

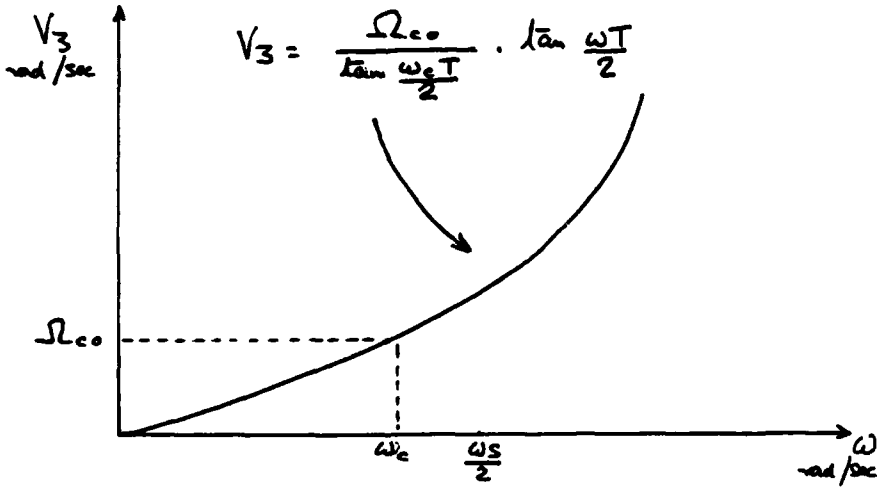

Fig A4d Warped frequencies (s-w_3 planes)

Fig A5

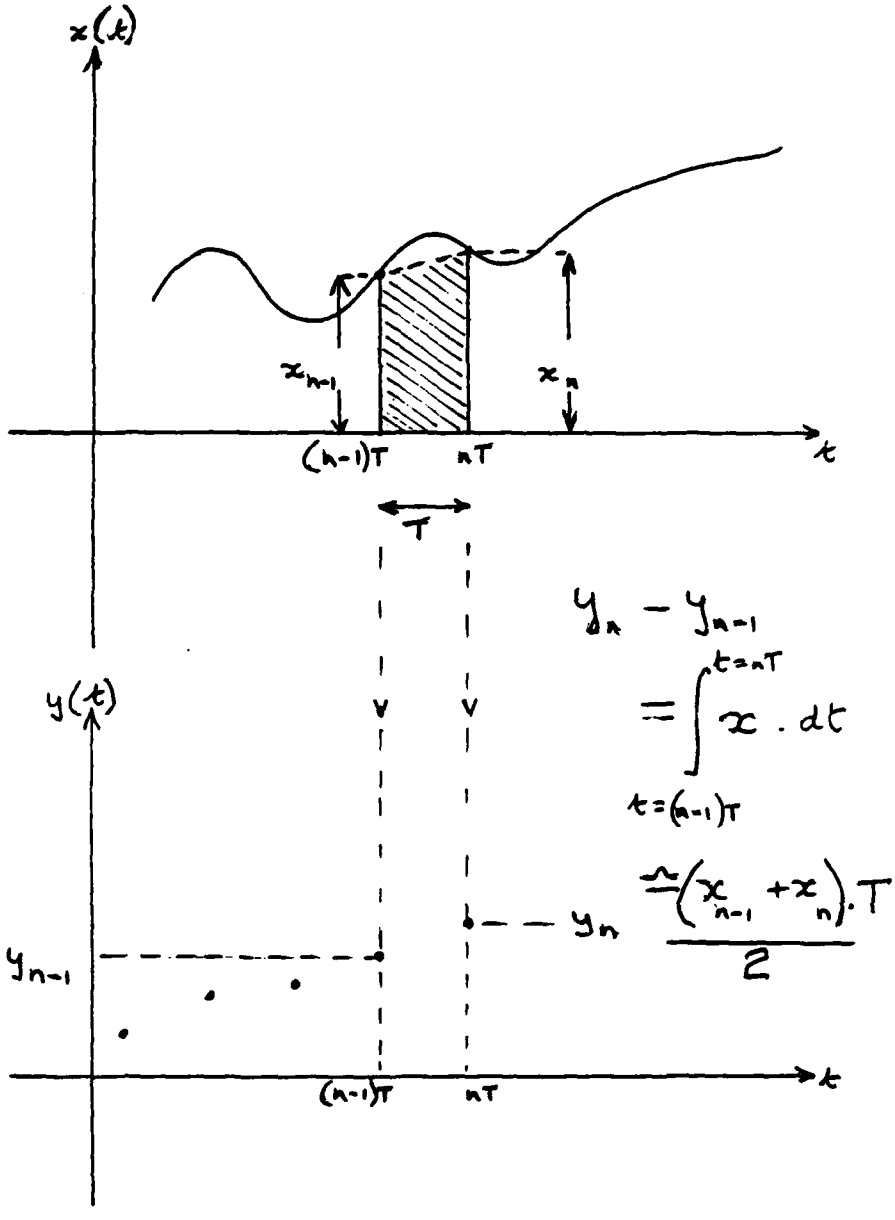

Fig A5 Trapezoidal approximation to integration

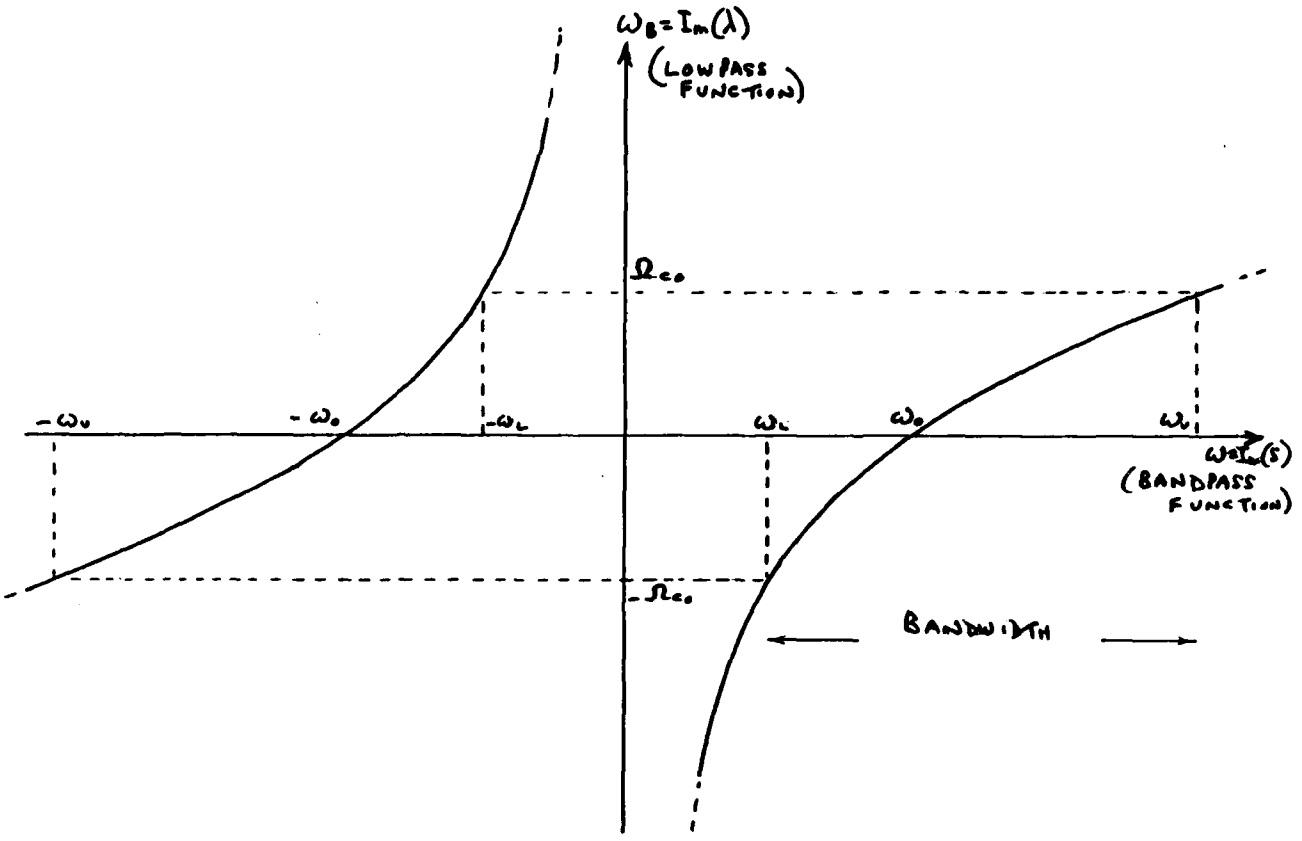

Fig A6 S-plane low pass to band-pass frequency transformation

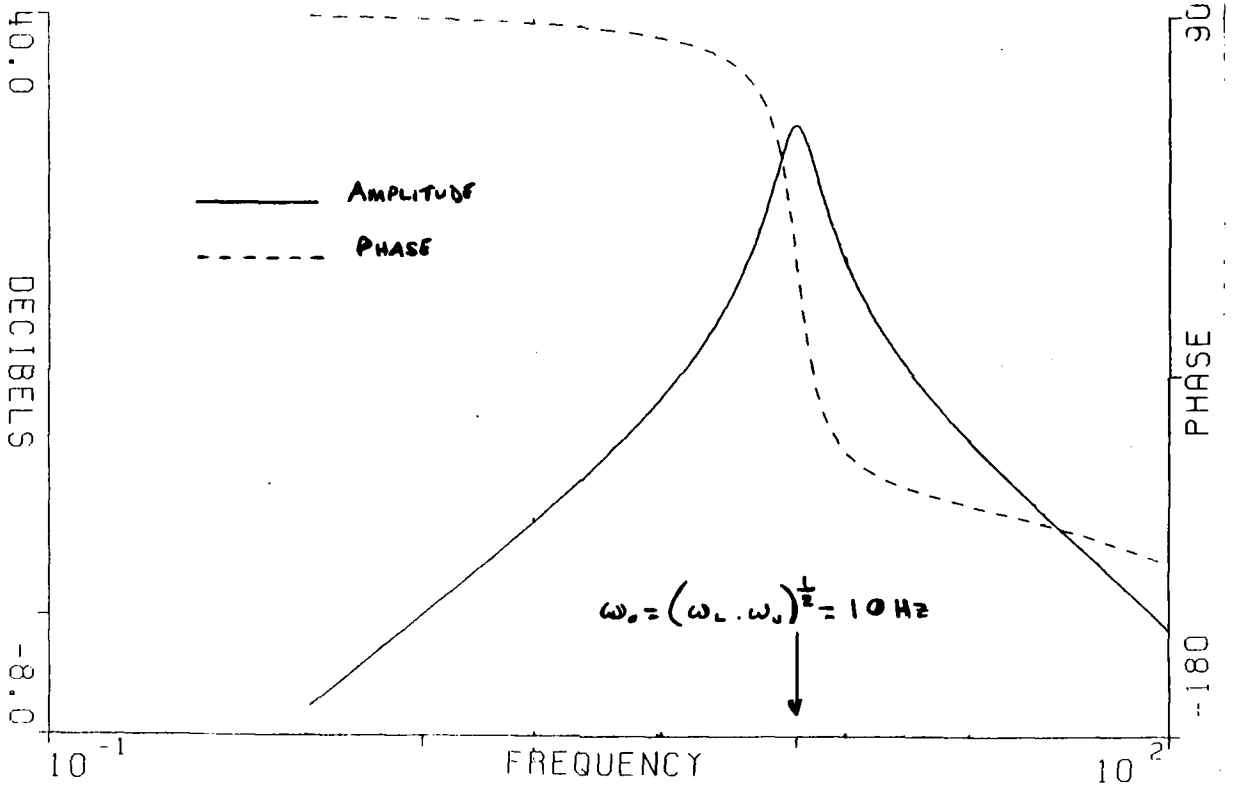

Fig A7

Fig A7 Band-pass characteristic $\dfrac{s(\omega_u - \omega_L)}{s^2 + s(\omega_u - \omega_L) + \omega_L\omega_u}$

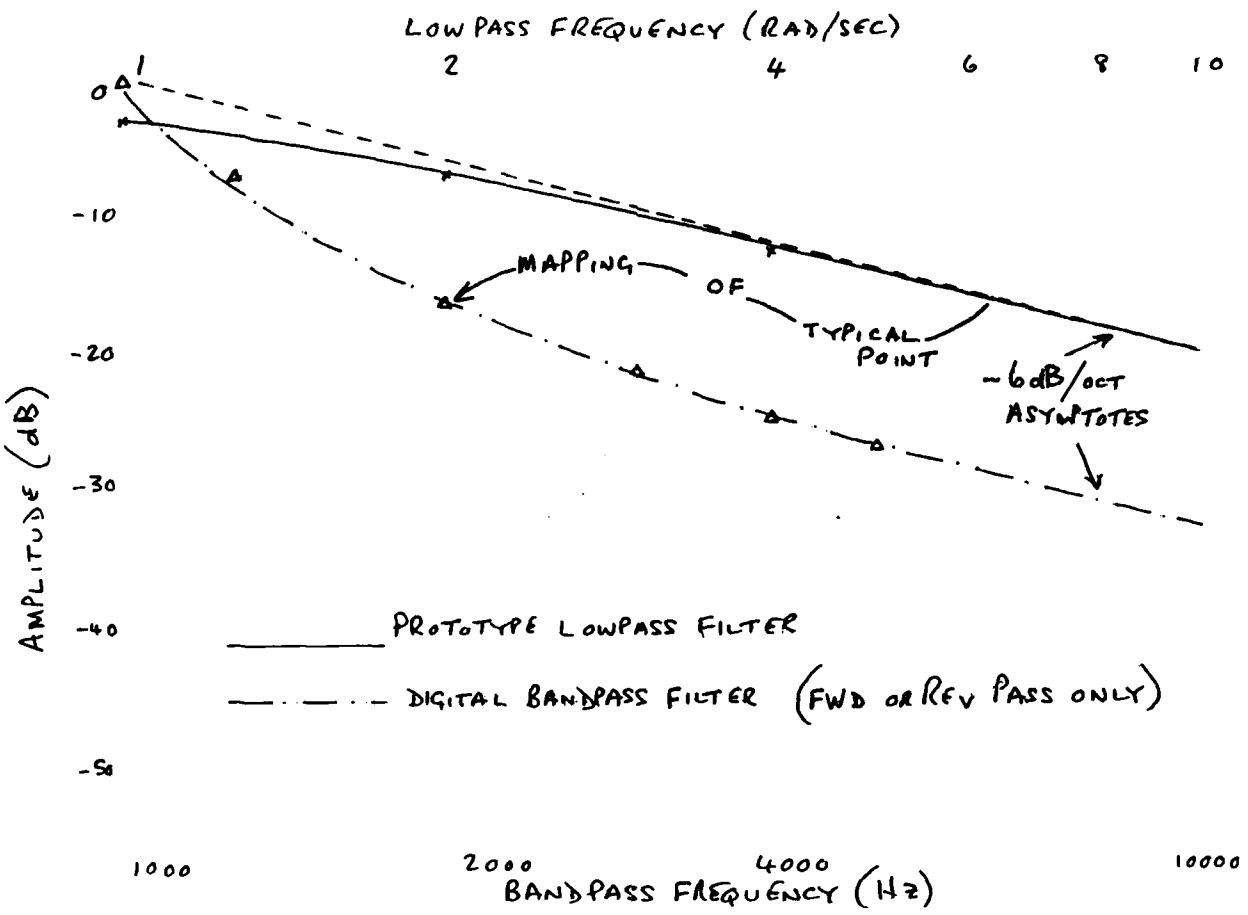

Fig A8 Final mapping of prototype low-nass continuous filter to digital bandpass filter